

## Anisotropy in Sickle Hemoglobin Fibers from Variations in Bending and Twist

M. S. Turner<sup>1\*</sup>, R. W. Briehl<sup>2</sup>, J. C. Wang<sup>2</sup>, F. A. Ferrone<sup>3</sup> and R. Josephs<sup>4</sup>

<sup>1</sup>*Department of Physics  
University of Warwick  
Coventry CV4 7AL, UK*

<sup>2</sup>*Department of Physiology  
& Biophysics, Albert Einstein  
College of Medicine, Bronx  
NY 10461, USA*

<sup>3</sup>*Department of Physics  
Drexel University, Philadelphia  
PA 19104, USA*

<sup>4</sup>*Department of Molecular  
Genetics & Cell Biology  
University of Chicago  
Chicago, IL 60637, USA*

We have studied the variations of twist and bend in sickle hemoglobin fibers. We find that these variations are consistent with an origin in equilibrium thermal fluctuations, which allows us to estimate the bending and torsional rigidities and effective corresponding material moduli. We measure bending by electron microscopy of frozen hydrated fibers and find that the bending persistence length, a measure of the length of fiber required before it starts to be significantly bent due to thermal fluctuations, is 130  $\mu\text{m}$ , somewhat shorter than that previously reported using light microscopy. The torsional persistence length, obtained by re-analysis of previously published experiments, is found to be only 2.5  $\mu\text{m}$ . Strikingly this means that the corresponding torsional rigidity of the fibers is only  $6 \times 10^{-27}$  J m, much less than their bending rigidity of  $5 \times 10^{-25}$  J m. For (normal) isotropic materials, one would instead expect these to be similar. Thus, we present the first quantitative evidence of a very significant material anisotropy in sickle hemoglobin fibers, as might arise from the difference between axial and lateral contacts within the fiber. We suggest that the relative softness of the fiber with respect to twist deformation contributes to the metastability of HbS fibers: HbS double strands are twisted in the fiber but not in the equilibrium crystalline state. Our measurements inform a theoretical model of the thermodynamic stability of fibers that takes account of both bending and extension/compression of hemoglobin (double) strands within the fiber.

© 2006 Elsevier Ltd. All rights reserved.

\*Corresponding author

*Keywords:* sickle; hemoglobin; fiber; macrofiber; fluctuations

### Introduction

The intracellular polymerization of deoxysickle cell hemoglobin (HbS,  $\beta 6 \text{ glu} \rightarrow \text{val}$ ) to form rod-like fibers is a primary cause of sickle cell anemia. The symptoms of the disease arise because cells containing fibers are rigid and pass through the capillary circulation with difficulty. Consequently, sickled cells may occlude the small capillaries causing local tissue destruction and extreme pain. Electron microscopy<sup>1–4</sup> and crystal X-ray diffraction<sup>5–7</sup> have established that the fiber consists of 14 strands of hemoglobin molecules twisted about a common axis with a pitch of about 2700 Å. The resulting helical fiber has a cross-section that is slightly elliptical (having an eccentricity of about 1.2) with a

mean radius of approximately 110 Å and a mean helical pitch length of approximately 2700 Å. The fibers grow to indefinite lengths, often tens of microns or longer. In addition to the damage arising as a direct result of red blood cell rigidification, there is now evidence that fiber assembly may now have a pathological effect on membrane function and ion balance.<sup>8</sup>

Ultimately, the pathology of the disease is controlled by the fibers that make the red cells rigid. This is, in turn, related to the mechanical properties of fibers, such as their intrinsic stiffness. The primary goal of the present study is to determine these mechanical properties. Ultimately, we would wish to be able to relate them to the bulk properties of HbS gels and sickled red cells. In particular, HbS gels may admit various torsional deformation modes and a knowledge of the torsional rigidity is therefore desirable to fully understand the mechanics and rheology of the gel. Additionally, we seek information on the unresolved issue of how and why HbS fibers form<sup>9</sup>

Abbreviations used: DIC, differential interference contrast; HbS, deoxysickle cell hemoglobin.

E-mail address of the corresponding author: [m.s.turner@warwick.ac.uk](mailto:m.s.turner@warwick.ac.uk)

rather than crystals since the fibers' spontaneous conversion to crystals implies that crystals are the more stable species.<sup>10–14</sup> The fact that we find that fibers are very soft with respect to twist deformation may provide a clue to understanding the transformation from helical polymers to fascicles and crystals.

Here we report on a study of the mechanics of fiber bending and twisting. Variations in bending and twisting are related to the relevant rigidities by utilizing elastic theory and the principle of equipartition of energy, which describes how all possible fluctuations are excited at thermal equilibrium.<sup>15</sup> This general approach has yielded the mechanical properties of several fluctuating biological structures<sup>16–18</sup> such as microtubules, actin and clathrin nets.

Bending fluctuations of HbS fibers have recently been observed by differential interference contrast (DIC) light microscopy.<sup>18</sup> The fluctuations can be easily observed using video microscopy and have correlation times of the order of seconds for fibers in the 10–20  $\mu\text{m}$  size range<sup>†</sup>. In this previous study, it was concluded that HbS fibers have a statistical persistence length of  $l_p = 240 \mu\text{m}$ , corresponding to a rigidity of  $\kappa = 1.0 \times 10^{-24} \text{ N m}^2$ . These quantities are, respectively, the “stiffness” length over which fiber orientation become uncorrelated due to thermal bending<sup>19</sup> and the constant relating stored energy per unit length to half the squared curvature<sup>20</sup> (analogous to the spring constant of a Hookian spring).

This earlier study did have certain limitations. In particular, since the DIC light microscope images were diffraction broadened, there was insufficient optical resolution for a reliable determination of whether single fibers or tight bundles of multiple fibers were present. Indeed there was quite strong evidence that fiber bundles were often present. Single fiber properties were inferred by suitable extrapolation. It was also not possible to study variations in fiber pitch because the optical resolution was inadequate to image the periodic variation in appearance that allows the pitch to be determined; the fibers appeared as featureless cylinders. In the present work, we overcome these limitations and report on a study of the fluctuations of individual frozen hydrated fibers by electron microscopy. Although individual fibers are frozen and immobile, viewing an ensemble of such fibers is equivalent to following the temporal variations of a single fiber. The electron micrographs have sufficient resolution to differentiate between individual fibers and bundles and to provide information on their helical pitch (twist).

Twisting and bending generate quite different internal strains in a fiber. For small deformations

bending involves pure axial extension/compression while twisting involves pure axial shear.<sup>20</sup> By studying both we will obtain two independent probes of the mechanical properties of the fiber.

## Bending Fluctuations

Information on the mechanical properties of HbS fibers can be obtained by studying their bending fluctuations. With this goal in mind, we studied frozen hydrated HbS fibers imaged by electron microscopy (see Table 1). We quantify the bending of each fiber by  $\delta u$ , the projection onto the focal plane of the normal deviation of its midpoint from the straight line joining its ends (see Figure 1). This is a quantitative measure of bending in so far as it can be related to the fiber rigidity  $\kappa$ , and hence the persistence length  $l_p = \kappa/k_B T$ <sup>19</sup> ( $k_B$  is Boltzmann's constant and  $T$  the absolute (lab) temperature). These quantities are, respectively, the constant relating stored energy per unit length to half the squared curvature<sup>20</sup> (analogous to the spring constant of a Hookian spring) and the “stiffness” length over which fiber orientations become uncorrelated due to thermal bending.

**Table 1.** The length and normal deviation at midpoint of each HbS fiber studied

Fiber number	Deviation at midpoint $\delta u$ (nm)	Length $L$ ( $\mu\text{m}$ )
1	–11.1	0.94
2	–7.1	1.09
3	7.1	0.72
4	4.0	0.74
5	–10.2	0.98
6	4.6	0.93
7	21.9	1.09
8	–22.2	1.23
9	–8.0	1.19
10	1.5	0.71
11	–4.9	1.16
12	10.4	1.29
13	0.0	1.49
14	24.0	0.95
15	–26.9	1.17
16	15.8	1.15
17	–25.7	1.16
18	29.9	1.49
19	12.7	0.99
20	4.8	0.37
21	–1.6	1.00
22	2.2	1.60
23	21.3	1.20
24	16.3	1.11
25	19.1	1.11
26	–13.6	1.39
27	–12.5	1.21
28	–5.2	0.83
29	7.8	1.14
30	–6.8	1.37
31	21.3	1.44

The average length of the fibers is  $\langle L \rangle = 1.10 \mu\text{m}$ . The fiber deviations are drawn from a distribution with zero mean and have a root mean squared magnitude  $\sqrt{\langle \delta u^2 \rangle} = 14.9 \text{ nm}$ .

<sup>†</sup> The longest correlation time is expected to be much shorter for the  $\sim 1 \mu\text{m}$  fibers of interest here, varying like the fourth power of their length.<sup>19</sup>

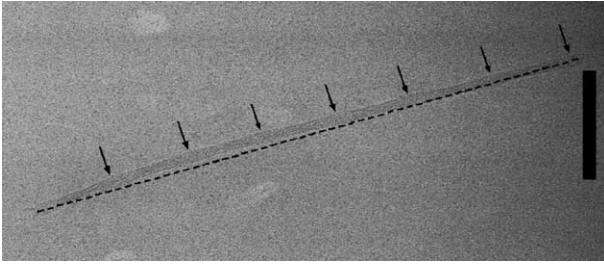


**Figure 1.** Electron micrograph of a typical frozen hydrated HbS fiber. The scale bar represents 0.2  $\mu\text{m}$ . The fiber is measurably bent with an 11.1 nm normal deviation at midpoint. The thickest parts of the fiber are separated by half a pitch length  $\lambda$  and are indicated by arrows. The distances between the indicated points along the fiber (from left to right) are 138 nm, 143 nm, 137 nm, 151 nm and 140 nm.

The bending energy  $H$  is related to  $\kappa$  as described above:

$$H = \frac{\kappa}{2} \int C(z)^2 dz \quad (1)$$

where  $z$  is the axial distance along the fiber and  $C$  its local curvature. The temperature prior to freezing (room temperature) determines the magnitude of the fluctuations since the fibers are frozen and immobilized extremely rapidly. In what follows it is convenient to define the rescaled fiber deviation at midpoint to be:

$$\Delta u = \frac{4\sqrt{3}}{L^{3/2}} \delta u \quad (2)$$

where  $L$  is the length of the fiber. Although not explicitly stated in an earlier study,<sup>18</sup> thermal bending fluctuations drive  $\Delta u$  to be distributed as a Gaussian random variable, i.e. with normal probability distribution. Furthermore, the distribution must have mean squared amplitude (variance)  $1/l_p$ . Adopting the notation that the average value of  $\Delta u^2$  is  $\langle \Delta u^2 \rangle$  we have:

$$l_p = 1/\langle \Delta u^2 \rangle \quad (3)$$

This is consistent with the distribution of our data (see Figure 2). This statement can be quantified by comparing the kurtosis, skewness and quartile skewness of the data with data drawn from a normal distribution with the same variance and zero mean. This procedure allows us to conclude that the data are consistent with a normal distribution at the 90% confidence level.

Thus, the variation in bending of the fibers is fully consistent with it having originated from thermal fluctuations.

### Results of analysis of bending

Elementary statistical analysis of the rescaled fiber deviations  $\Delta u$  (see Figure 2) yields a best

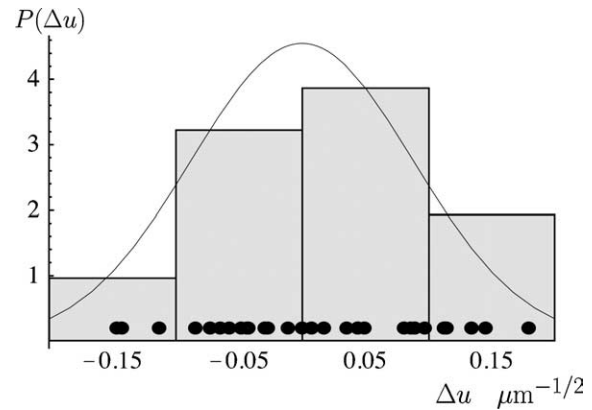


**Figure 2.** The distribution of fiber deviations is consistent with thermal Gaussian fluctuations. The solid disks represent the measured value of the rescaled fiber deviation at midpoint  $\Delta u = 4\sqrt{3} L^{-3/2} \delta u$  for each fiber. This quantifies the bending fluctuations of the fibers and at equilibrium is predicted to be a Gaussian random variable with mean zero and mean-squared value (variance)  $\langle \Delta u^2 \rangle = 1/l_p = 1/130 \mu\text{m}^{-1}$ . A normalized Gaussian probability distribution  $P(\Delta u) \propto \exp[-\Delta u^2/2\langle \Delta u^2 \rangle]$  is shown (continuous curve) together with a histogram of the data. Given that each fiber is subject to an arbitrary rotation, and hence choice of sign of  $\Delta u$ , the data are drawn from a distribution with zero mean.

estimate of  $l_p$  from equation (3):

$$l_p = 130 \mu\text{m} \quad \kappa = 5.2 \times 10^{-25} \text{ N m}^2 \quad (4)$$

We compute the  $\chi^2$  confidence intervals at the 90% level to be  $81 \mu\text{m} < l_p < 191 \mu\text{m}$  and  $3.2 \times 10^{-25} \text{ N m}^2 < \kappa < 7.7 \times 10^{-25} \text{ N m}^2$ . This confidence interval overlaps with an earlier estimate of the bending rigidity<sup>18</sup> which has a corresponding  $\chi^2$  confidence interval at the 90% level of  $184 \mu\text{m} < l_p < 278 \mu\text{m}$ .

Under the assumption that the fiber is made up of a uniform elastic medium the extensional modulus of the material  $E$  can be obtained from  $E = 4l_p kT/(\pi b_1^2 b_2^2)$  where  $b_1$  and  $b_2$  are the semimajor and semiminor axes of the elliptical cross-section. Using the consensus literature values<sup>21,22</sup>  $b_1 = 120 \text{ \AA}$  and  $b_2 = 95 \text{ \AA}$  we thereby obtain an estimate of the extensional modulus of the fiber material  $E = 51 \text{ MPa}$ .

### Twist Fluctuations

As discussed above, HbS fibers are known to be helical, with an average pitch length of approximately  $2\lambda = 2700 \text{ \AA}$ . Thus, in the absence of any variations in twist, the elliptical shape of the fiber cross-section rotates through an angle of  $\pi$  radians ( $180^\circ$ ) over one half pitch length  $\lambda$  of the fiber. In this case, the torsional elastic energy stored in a helical fiber is zero. We can express this mathematically as  $\frac{d\theta}{dx} = \pi/\lambda$  where the orientation of the

fiber cross-section  $\theta(x)$  is a function of its position along the fiber, here taken to define the  $x$ -axis.

In order to understand the stored elastic energy due to variations in local twist we define the local "overtwist:"

$$\tau = \frac{d\theta}{dx} - \frac{\pi}{\lambda} \quad (5)$$

which can be either positive (overtwist) or negative (undertwist).

The elastic energy stored in a homogenous fiber when it is subject to variations in twist involves this overtwist. We propose that it is well approximated by:

$$H = \frac{c}{2} \int \left( \tau(x)^2 + l^2 \left( \frac{d\tau}{dx} \right)^2 \right) dx \quad (6)$$

where the integral is over the entire length of the fiber and  $c$  is a torsional rigidity which controls the stiffness of the fiber with respect to twisting motion. For  $l=0$  this expression reduces to a version of Hooke's law, which states that stored energy is proportional to the squared strain,<sup>20</sup> up to a trivial identification of strain with the overtwist, rather than actual twist. In fact,  $l$  is always non-zero and is the range of spatial correlations in twist, of the scale of a few molecular repeats.<sup>3</sup> Thus, for two segments of the fiber separated by much more than  $l$ , the local twist at one point gives no information about the twist at the other point.

Equation (6) represents the leading order terms in an expansion in powers and derivatives of the twist and remains accurate provided that the fiber can be described as a continuous medium and the strains are small, as we expect to be the case here. It basically amounts to treating the deformation modes of the fiber in the simplest possible way: as if they were (generalized) springs with a restoring force that is proportional to the strain. Equation (6) is known as the Gaussian model within statistical field theory<sup>23</sup> and several well-known results stem from it, as we will exploit.

### Torsional rigidity from data for variations in pitch length

We aim first to show how a description of the fiber based on equation (6) can be used to relate the observed variations in twist per half pitch length to the torsional rigidity  $c$ . This will then be compared with the estimate of bending rigidity  $\kappa$  obtained from our analysis of bending variations. For a uniform "isotropic" elastic medium one would expect these to be very similar.<sup>20</sup> We will show that in fact our estimates of  $c$  and  $\kappa$  differ by two orders of magnitude as would reflect a material with significant anisotropy.

We analyze data<sup>3,24</sup> for the mean squared deviation in half pitch length  $\langle \Delta\lambda^2 \rangle$  which, for small deviations  $\langle \Delta\lambda^2 \rangle \ll \lambda^2$ , we assert can be related

to the twist according to:

$$\langle \Delta\lambda^2 \rangle = \left( \frac{\lambda}{\pi} \right)^2 \left\langle \int_x^{x+\lambda} \tau(x') dx' \int_x^{x+\lambda} \tau(x'') dx'' \right\rangle \quad (7)$$

To understand this consider that the integrated (total) angular overtwist for a section of length  $\lambda$  is  $\Delta\theta = \int_x^{x+\lambda} \tau(x') dx'$ . This translates to a variation in pitch length of  $\Delta\lambda = \lambda\Delta\theta/\pi$ , the mean-squared value of which is given by equation (7). By exploiting the principle of equipartition of energy<sup>25</sup> on equation (6), equivalent to assuming local thermodynamic equilibrium, we find that equation (7) can be solved exactly:

$$\langle \Delta\lambda^2 \rangle = \frac{k_B T \lambda^3}{c \pi^2} \left[ 1 - \frac{l}{\lambda} (1 - e^{-\lambda/l}) \right] \quad (8)$$

This expression reduces to  $\langle \Delta\lambda^2 \rangle = \frac{k_B T \lambda^3}{c \pi^2}$  when  $\lambda \gg l$ . This result can be used to extract the torsional rigidity from data for the variations in the pitch length. For negatively stained fibers<sup>3</sup> it was reported that the mean pitch length was  $\langle \lambda \rangle = 1349 \text{ \AA}$  with variations that displayed an approximately normal distribution with root mean squared variation  $\sqrt{\langle \Delta\lambda^2 \rangle} = 88 \text{ \AA}$ . Similar numbers were reported for frozen hydrated fibers<sup>24</sup> for which  $\langle \lambda \rangle = 1445 \text{ \AA}$  and  $\sqrt{\langle \Delta\lambda^2 \rangle} = 131 \text{ \AA}$ . From equation (8) (with  $\lambda = \langle \lambda \rangle$ ) we obtain estimates of the torsional rigidity  $c$  and the torsional persistence length  $l_c$  of  $l_c = c/k_B T = 3.2 \text{ \mu m}$  for the negatively stained fibers<sup>3</sup> and  $l_c = c/k_B T = 1.8 \text{ \mu m}$  for the frozen hydrated fibers.<sup>24</sup> A simple average of these values gives:

$$l_c = c/k_B T = 2.5 \text{ \mu m} \quad c = 6.0 \times 10^{-27} \text{ J m} \quad (9)$$

## Discussion and Conclusions

We find that the torsional rigidity  $c = 2.5 k_B T \mu\text{m}$  obtained from the analysis of twisting, is much smaller than the bending rigidity  $\kappa = 130 k_B T \mu\text{m}$  obtained from an analysis of bending variations. As mentioned above for a uniform "isotropic" elastic medium one would expect these to be rather similar.

There are two possible factors that may contribute to this discrepancy and both may be present to some extent: first, the fiber may be comprised of a highly anisotropic elastic medium. In this case, the axial shear response is much softer than the extension/compression in a way that we are able to quantify in terms of two effective moduli. This anisotropy might be explained on the grounds that the contacts which stabilize the double strands (which run nearly parallel with the fiber axis) are thought to be stronger than the inter double strand contacts which are primarily radial.

The possibility remains that the fiber may contain plastic-like twist deformations. These would correspond to packing disorder or variations likely

frozen-in at fiber assembly. They could therefore reflect kinetic, rather than thermodynamic, effects. In this case, the observed torsional variations may not be entirely thermal in origin but might instead reflect a torsional energy, which is anharmonic, perhaps with more than one locally metastable configuration. While we cannot entirely rule out the possibility that such hypothetical plastic deformations may be present we are encouraged by the fact that a theoretical estimate for the torsional rigidity that includes no such plastic deformations<sup>26</sup> is in extremely close agreement with the value that we have here obtained from experimental data. This agreement supports our assumption that the variations are largely due to thermal variations in (over)twist.

The sickle hemoglobin fibers which contain 14 strands are known to have different contact regions along the axis of the fiber and in the diagonal contacts between nearest lateral neighbors, and it is likely the differences between these types of contacts that give rise to the anisotropy reported here. Our prediction that HbS fibers are extremely soft with respect to twist deformation may be highly significant in understanding the overall metastability of HbS fibers. Fibers are known to be metastable with respect to the equilibrium crystal phase, which consists of a crystalline array of "untwisted" double strands of HbS molecules.<sup>27</sup> The anisotropy we report here for the first time provides an explanation of this metastability in terms of a correspondingly low energy cost to form twisted bundles. In an accompanying paper,<sup>26</sup> we have used our estimate of the extensional modulus to construct a model for the free energy, and hence the thermodynamic stability, of fibers and macro-fibers.

## Methods

### Fibers used for measuring bending

Fibers were dispersed on a copper electron microscope grid before rapid freezing in liquid ethane (which immobilizes them). To describe this in more detail a thin layer of an aqueous solution containing fibers is layered over the carbon film. The aqueous film is extremely thin being only approximately twice as thick as the sickle hemoglobin fiber itself. Some of the solution is suspended over the holes so the fibers can be imaged without the carbon film perturbing their structure. The grid is plunged into liquid ethane ( $-170^{\circ}\text{C}$ ) at a velocity of approximately 2 m/s. Thus, it takes 1.5 ms for the entire grid to become immersed in the liquid ethane. However, our interest is in suspended fibers that occupy only 1  $\mu\text{m}$  or so of the grid. A 1  $\mu\text{m}$  long region would be immersed in the liquid ethane in approximately 1.6  $\mu\text{s}$ , far faster than the  $\sim 1$  ms longest bending relaxation time for a 1  $\mu\text{m}$  length semiflexible polymer in water.<sup>19</sup>

After freezing the grids are maintained at  $-170^{\circ}\text{C}$  in liquid nitrogen and are examined in the electron microscope using a holder (Gatan 626 cryoholder) which also maintains the specimen at  $-170^{\circ}\text{C}$ . Only fibers that were not touching any other fiber or object

and whose full length was contained in the micrograph were selected for analysis. Grids were covered with a fenestrated (holey) carbon film. Only fibers that were suspended over the holes were selected, since only for these fibers could one be certain that they were not touching any other object. These criteria ensure that only fibers suspended freely in solution were included in our analysis. Experiments involving negatively stained fibers lying on the carbon support film were not used for bending measurements, since contact with the supporting film could affect their profile. The fact that HbS fibers have elliptical cross-sections motivates us to study fibers with lengths much larger than one half pitch length as the observed fluctuations of shorter fragments may depend on their orientation on the grid.

### Fibers used for measuring variations in twist

HbS fibers have an elliptical cross-section with major and minor diameters of 25 nm and 20 nm. Consequently, in lateral views, the particle width alternates between 25 nm and 20 nm. Because these wide and narrow regions repeat every  $180^{\circ}$  of rotation along the length of the particle, the average pitch of the fiber can be determined by measuring the distance between successive wide (or narrow) regions. Such measurements show that the distance between narrow regions (or wide regions) varies from fiber to fiber and along the length of individual fibers, and have established that HbS fibers have a variable pitch. One consequence of a variable pitch is that the axial rotation between hemoglobin molecules also varies. The axial rotation between HbS molecules in a fiber has been determined.<sup>2,3</sup> In those studies, fibers were absorbed to a carbon film and negatively stained. Negative staining will not modify the fiber twist significantly if adherence to the carbon film does not involve rotational forces. The similarity between results obtained from negatively stained and frozen hydrated fibers suggests that this is the case.

## Acknowledgements

This work was supported by the National Institutes of Health (NHLBI) program project grant HL 58512 (to R.W.B. (PI), F.A.F. and R.J.) and grant HL22654 (to R.J.).

## References

1. Dykes, G., Crepeau, R. H. & Edelstein, S. J. (1979). Three-dimensional reconstruction of the 14-filament fibers of hemoglobin S. *J. Mol. Biol.* **130**, 451–472.
2. Bluemke, D. A., Carragher, B. & Josephs, R. (1988). The reconstruction of helical particles with variable pitch. *Ultramicroscopy*, **26**, 255–270.
3. Carragher, B., Blumeke, D. A., Gabriel, B., Potel, M. J. & Josephs, R. (1988). Structural analysis of polymers of sickle cell hemoglobin. *J. Mol. Biol.* **199**, 315–331.
4. Dykes, G., Crepeau, R. H. & Edelstein, S. J. (1978). Three-dimensional reconstruction of the fibres of sickle cell haemoglobin. *Nature*, **272**, 506–510.
5. Wishner, B. C., Ward, K. B., Lattman, E. E. & Love, W. E. (1975). Crystal structure of sickle-cell deoxyhemoglobin at 5 Å resolution. *J. Mol. Biol.* **98**, 179–198.

6. Padlan, E. & Love, W. E. (1985). Refined crystal structure of deoxyhemoglobin S. *J. Biol. Chem.* **260**, 8272–8285.
7. Harrington, D. J., Adachi, K. & Royer, W. E. (1997). The high resolution crystal structure of deoxyhemoglobin S. *J. Mol. Biol.* **272**, 398–407.
8. Bookchin, R. M., Etzion, Z., Sorette, M., Mohandas, N., Skepper, J. N. & Lew, V. L. (2000). Identification and characterization of a newly recognized population of high- $\text{Na}^+$ , low- $\text{K}^+$ , low-density sickle and normal red cells. *Proc. Natl Acad. Sci. USA*, **97**, 8045–8050.
9. Makowski, L. & Magdoff-Fairchild, B. (1986). Polymorphism of sickle cell hemoglobin aggregates: structural basis for limited radial growth. *Science*, **234**, 1228–1231.
10. Pumphrey, J. G. & Steinhardt, J. (1977). Crystallization of sickle hemoglobin from gently agitated solutions—an alternative to gelation. *J. Mol. Biol.* **112**, 359–375.
11. Jones, M. M. & Steinhardt, J. (1979). Thermodynamic study of the crystallization of sickle-cell deoxyhemoglobin (hemoglobin s solubility, saturation concentration, enthalpy of crystallization, entropy of crystallization). *J. Mol. Biol.* **129**, 83–91.
12. Wellem, T. E. & Josep, R. (1979). Crystallization of sickle cell hemoglobin by fiber alignment and fusion. *J. Mol. Biol.* **135**, 651–674.
13. Wellem, T. E. & Josep, R. (1980). Helical crystals of sickle cell hemoglobin. *J. Mol. Biol.* **137**, 443.
14. Wellem, T. E. & Josep, R. (1981). Polymorphic assemblies of double strands of sickle cell hemoglobin: manifold pathways of deoxyhemoglobin S crystallization. *J. Mol. Biol.* **153**, 1011–1026.
15. Landau, L. D. & Lifshitz, E. M. (1986). *Statistical Physics*, Butterworth-Heinemann, Oxford, UK.
16. Jin, A. J. & Nossal, R. (2000). Rigidity of triskelion arms and clathrin nets. *Biophys. J.* **78**, 1183–1194.
17. Gittes, F., Mickey, B., Nettleton, J. & Howard, J. (1993). Flexural rigidity of microtubules and actin filaments measured from thermal fluctuations in shape. *J. Cell Biol.* **120**, 923–934.
18. Wang, J. C., Turner, M. S., Agarwal, G., Kwong, S., Josep, R., Ferrone, F. A. & Briehl, R. W. (2002). Micromechanics of isolated sickle hemoglobin fibers: bending moduli and persistence lengths. *J. Mol. Biol.* **315**, 601–612.
19. Doi, M. & Edwards, S. F. (1986). *The Theory of Polymer Dynamics*, Oxford University Press, Oxford, UK.
20. Landau, L. D. & Lifshitz, E. M. (1986). *Theory of Elasticity*, Butterworth-Heinemann, Oxford, UK.
21. Wang, Z., Kishchenko, G., Chen, Y. & Josep, R. (2000). Polymerization of deoxy-sickle hemoglobin in high phosphate buffer. *J. Struct. Biol.* **131**, 197–209.
22. Watowich, S. J., Gross, L. J. & Josep, R. (1993). Analysis of the intermolecular contact sites within sickle hemoglobin fibers: effect of site-specific substitutions, fiber pitch and double strand disorder. *J. Struct. Biol.* **111**, 161–179.
23. le Bellac, M. (1991). *Quantum and Statistical Field Theory*, Oxford University Press, Oxford, UK.
24. Lewis, M. R., Gross, L. J. & Josep, R. (1994). Cryo-electron microscopy of deoxy-sickle hemoglobin fibers. *Microsc. Res. Tech.* **27**, 459–467.
25. Chaikin, P. M. & Lubensky, T. C. (1997). *Principles of Condensed Matter Physics*, Cambridge University Press, Cambridge, UK.
26. Turner, M. S., Ferrone, F. A., Briehl, R. W. & Josep, R. (2003). Twisted protein aggregates and disease: the stability of sickle hemoglobin fibers. *Phys. Rev. Letters*, **90**, 128103.
27. Jones, M. M. & Steinhardt, J. (1979). Thermodynamic study of the crystallization of sickle-cell deoxyhemoglobin (hemoglobin's solubility/saturation concentration/enthalpy of crystallization/entropy of crystallization). *J. Mol. Biol.* **129**, 83–91.

Edited by I. B. Holland

(Received 1 September 2005; received in revised form 17 January 2006; accepted 18 January 2006)  
Available online 6 February 2006